

# Analysis of bandwidth measurement methodologies over WLAN systems

Marc Portoles-Comeras

Centre Tecnològic de Telecomunicacions de  
Catalunya (CTTC)  
Castelldefels (Barcelona), Spain  
mportoles@ctt.cat

Josep Mangués-Bafalluy

Centre Tecnològic de Telecomunicacions de  
Catalunya (CTTC)  
Castelldefels (Barcelona), Spain  
jmangués@ctt.cat

Albert Cabellos-Aparicio

Universitat Politècnica de Catalunya  
Barcelona, Spain  
acabello@ac.upc.edu

Jordi Domingo-Pascual

Universitat Politècnica de Catalunya  
Barcelona, Spain  
acabello@ac.upc.edu

## ABSTRACT

WLAN devices have become a fundamental component of nowadays network deployments. However, even though traditional networking applications run mostly unchanged over wireless links, the actual interaction between these applications and the dynamics of wireless transmissions is not yet fully understood. An important example of such applications are bandwidth estimation tools. This area has become a mature research topic with well-developed results. Unfortunately recent studies have shown that the application of these results to WLAN links is not straightforward. The main reasons for this is that the assumptions taken to develop bandwidth measurements tools do not hold any longer in the presence of wireless links (e.g. non-FIFO scheduling). This paper builds from these observations and its main goal is to analyze the interaction between probe packets and WLAN transmissions in bandwidth estimation processes. The paper proposes an analytical model that better accounts for the particularities of WLAN links. The model is validated through extensive experimentation and simulation and reveals that (1) the distribution of the delay to transmit probing packets is not the same for the whole probing sequence, this biases the measurements process and (2) existing tools and techniques point at the achievable throughput rather than the available bandwidth or the capacity, as previously assumed.

## Keywords

Bandwidth Measurements, WLANs, Random Access, Bandwidth Metrics

## 1. INTRODUCTION

WLAN devices have become a fundamental component of nowadays network deployments. They can be found in scenarios that range from simple home networks to complex mesh-like multi-radio multi-hop in-

frastructures. However, even though traditional networking applications run mostly unchanged over wireless links, the actual interaction between these applications and the dynamics of wireless transmissions is not yet fully understood.

Bandwidth measurement tools and techniques are an example of such applications. Bandwidth measurements have become a mature research topic with well-developed results both at a practical level (e.g. [1, 17, 18, 19, 20, 22, 23]) and, lately, at a more fundamental level [13, 14]. However, various preliminary studies have shown that the application of these results to WLAN environments is not straightforward ([2, 3]).

The main reasons for this reside on the assumptions taken to develop bandwidth measurement models and tools. On one side, traditional active measurement techniques are based on the concept of a single bit-carrier multiplexing several users in FIFO order (e.g. [1]). Additionally, it is commonly assumed that communication links present a constant transmission rate along the measurement process. Further, another common assumption to take is that the impact of low-layer overheads can be neglected and measurements taken with a given packet size can be easily extended to packets of different sizes.

These assumptions do not hold any longer in the presence of wireless links. First, multiple-user access schemes such as the CSMA/CA compromise the FIFO assumption [3]. Second, the service rate may change along the measurement process [7]. Finally, previous studies [3, 4] have shown that bandwidth metrics of a wireless link cannot be easily normalized and that measurements have to take into account the packet size used.

This paper builds from these observations in order to analyze the interaction between probe packets and

WLAN transmissions in active measurement processes. Specifically, the paper proposes a model that better accounts for the particularities of wireless links. The model is validated through extensive experimentation and simulation and is used to derive the specific dynamics of probing packets in the presence of WLAN links. The model is then used to obtain a complete characterization of bandwidth measurements gathered using active probing sequences. The paper presents both fluid and non-fluid approaches to the bandwidth measurement problem. For the non-fluid approach we extend a recently developed mathematical framework [13] to cope with the specificities of WLAN transmissions.

The contributions of the paper are the following:

- First, it reveals how the distribution process describing the delay to transmit probing packets in a WLAN system is not the same for the whole probing sequence. Instead, the distribution follows a transitory regime before reaching a stationary state.
- Second, taking a fluid approach to the bandwidth measurement problem, it shows that traditional tools point at the *achievable throughput*, rather than the *available bandwidth* or the *capacity* when applied over wireless links.
- Third, it shows how dispersion based measurements based on a short number of probing packets are biased measurements of the *achievable throughput*. The origin of this bias lies on the transitory detected in the service delay of probing packets.

The results described here have several consequences that transcend the scope of the paper and can be useful to the research community. First, we show how the packet pair technique [23], widely used in the wireless mesh routing literature [21], constitutes a biased measure of the *achievable throughput*. We show also that it can only be used to measure the transmission rate of a wireless link in a very particular circumstance (i.e. when there is no contending traffic). Second, we introduce a simple yet effective method to improve the accuracy and convergence properties of bandwidth measurement tools. Interestingly this method not only improves measurements in wireless scenarios but also in wired ones.

The rest of the paper is organized as follows. Section 2 introduces the tools that have been used throughout the paper in order to validate results. Section 3 introduces the proposed model for WLAN links. The model is validated with extensive measurements. Section 4 introduces the basics of bandwidth measurement over WLANs and presents results when taking a fluid approximation to the problem. Section 5 relaxes the fluid approximation, adapts a recent analysis framework

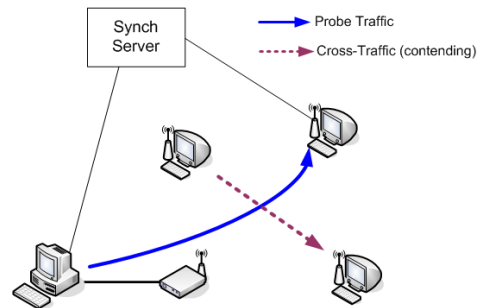


Figure 1: Experimental/simulation scenario

to the specificities of WLAN transmissions and derives possible biases in the results of the measurement process when using dispersion based techniques. Section 6 discusses the consequences of some of the findings presented. Finally, section 7 concludes the paper.

## 2. VALIDATION SETUP

The study presented in this section is based on theoretical analysis, simulation and experimentation. This section introduces the simulation and experimentation settings used to gather measurement data and validate theoretical findings.

Experimentation has been carried out within the EXTREME framework (see [9]). This is a multi-purpose networking experimental platform. The main advantage of this platform is its high automation capabilities that allow automatic execution, data collection and data processing of several repetitions of an experiment.

The WLAN devices used are Z-COM ZDC XI-626 cards which carry the popular Prism chipset. These wireless devices are controlled using computer nodes of the EXTREME cluster. In all cases these nodes are Pentium IV PCs with a 3GHz processor, 512MB of RAM memory and running Linux OS, with kernel 2.4.26. To control these devices, the EXTREME automation system makes use of the wireless extensions API.

In order to generate the traffic (probing and cross-traffic), we make use of the Multi-GENerator toolset [10]. However, in order to increase the accuracy of the time-stamping procedure, both at sender and receiver sides, network device drivers have been conveniently modified to timestamp packets just before they are laid down to the hardware (sending side) and just after getting them from the hardware (receiving side). This follows some of the ideas described in [11].

Figure 1 shows the basic setup used throughout the section for experimentation. The probing traffic is sent between two stations that are conveniently synchronized. This synchronization is achieved by sending frequent NTP updates through a parallel wired interface between the NTP server and the measurement nodes.

Using this method we achieve accuracies of delay measurement in the order of ten microseconds.

Unless specified the cross-traffic generated follows a Poisson distribution.

Some of the experiments required a large amount of repetitions to achieve accurate convergence of results. Since this is difficult to achieve in a testbed we have also used a simulator. Specifically we have replicated the testbed (figure 1) using NS2 (ver. 2.29 [12]). The main difference between the testbed and the simulator is that the latter includes scenarios with up to 5 contending nodes. Following some recent research results [24] both the testbed and the simulator went through a thorough calibration process in order to assure that the results gathered are comparable.

The simulator uses the NO Ad-Hoc Routing Agent. This agent supports static routing configurations over wireless networks and does not send any routing related packets. This avoids possible interferences with probe or cross-traffic. Regarding the configuration, all the experiments use the default MAC and PHY 802.11 layers included into the NS2 package. The queues used are infinite, this way we avoid dealing with packet losses, which are irrelevant for our study. Finally all the wireless nodes are static and equally spaced from the Access Point. The physical transmission rate is set to 11Mbps and RTS/CTS is not used.

Finally, we have also developed a queuing simulator using Matlab. The motivation for this is that the probing process in a WLAN presents multiple components that are difficult to isolate from each other in an experimentation setting or even through simulations. The queuing simulator convolves a series of packet arrivals with a series of service times in order to measure several metrics such as the queuing length distribution and the output dispersion (inter-arrival) of packets. The input parameters are gathered from experimentation measurements in order to keep the results as close to the real behavior as possible.

Unless noted otherwise the results presented in this work have been obtained from repeating experiments over 80 times while the simulations have been repeated 25.000 (NS2) to 70.000 (Matlab) times.

### 3. MODEL OF WLANS FOR BANDWIDTH MEASUREMENTS

Traditionally the development of bandwidth measurement techniques rely on a series of well-accepted assumptions. However some of them do not hold true in the presence of wireless links. This section reviews these assumptions, proposes a more generic model accounting for WLAN specificities and validates the model through extensive measurements.

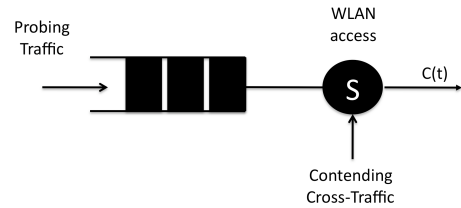


**Figure 2: Model of the interaction between probing traffic and (contending) cross-traffic in a WLAN system**

#### 3.1 Model of a WLAN link

Developments related to bandwidth measurements usually rely on three assumptions that cannot be taken in WLAN environments. First, a vast majority of studies consider network links as single bit-carriers that multiplex multiple users in FIFO order [1]. Second, it is commonly assumed that communication links present a constant (fixed) transmission rate along the measurement time. Third, the impact of low-layer overheads is usually neglected and tools are developed considering that results gathered with packets of a given size can be extended to other sizes.

Firstly, Multiple-access schemes related to WLAN links prevent taking the FIFO assumption of traditional models. As a result of using techniques such as the DCF mechanism in the IEEE 802.11 MAC protocol, probing traffic and cross-traffic are scheduled to use the channel in a non-FIFO manner [3]. A consequence of this is that the delay that packets experience once they are at the head of the transmission queue until they are completely transmitted becomes a random process. This random process depends on the amount of traffic contending for channel access at every instant and the specific scheduling algorithm used.

Additionally, the variability of wireless channels and the protection mechanisms usually adopted invalidate the assumption of a constant transmission rate. ARQ mechanisms or rate adaptation strategies change the amount of time necessary to transmit a given packet in case of a variation in channel propagation conditions. Hence breaking the assumption of a constant transmission rate [7]. Again, as a consequence, the delay to service packets at the head of the transmission queue becomes a random process.

Finally, recent studies [3, 4] have shown that in WLAN environments bandwidth measurements taken with packets of a given size cannot be easily extended to other packet sizes. The origin of this are the large low layer overheads associated to WLAN transmissions. This assumption was usually used to normalize both probe traffic and cross-traffic to a common unit (i.e bits per second) and led developing measurement tools irrespec-

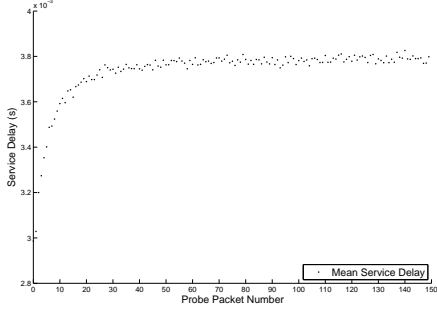


**Figure 3: Mean Service Delay vs. Probe packet num**

tive of the packet size used. In WLANs the interaction between cross-traffic and probing traffic cannot be normalized to bits per second. Instead it has to be studied from the perspective of time (transmission time, channel utilization time, scheduling delay, etc.).

Taking all these observations into account, figure 2 presents the model used all along the paper. Probing packets enter a transmission queue and get service in FIFO order. Once at the head of the transmission queue, they suffer a random transmission delay associated to the scheduling mechanism and/or variations of channel propagation characteristics. As it can be noted cross-traffic that contends for channel access is not considered from a packet or bit per second perspective but it is included in the random service delay that probing packets suffer.

This model is non-parametric, hence it does not make any assumption about the distribution of the service delay of probing packets.

### 3.2 Analysis of service delay

This section analyses the characteristics of the service delay that probe packets experience. We take as service delay the time since the probing packet is ready to be transmitted (it is at the head of the transmission queue in figure 2) until it is completely transmitted. The service delay in WLANs has been repeatedly studied in the literature. Indeed, different researchers have analyzed its exact distribution using stochastic tools, such as Markov Chains [5, 8], others show how the exponential distribution provides a good fit [6]. All these studies have focused on the distribution of the service delay in *stationary* state. However, in general, bandwidth measurements are gathered using packet trains with a limited length (limited number of packets). As a consequence, for the purpose of this work, we are interested in analyzing how the service delay evolves over time as an increasing number of probing packets are sent through the WLAN.

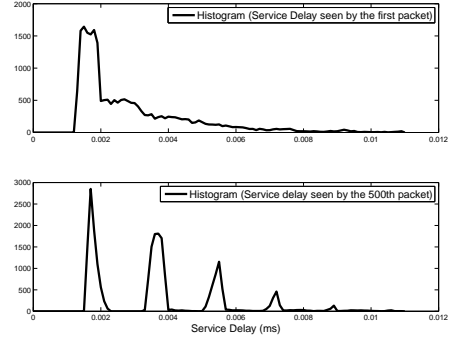


**Figure 4: Histogram of the s.d seen by the first and 500th packet (simulation)**

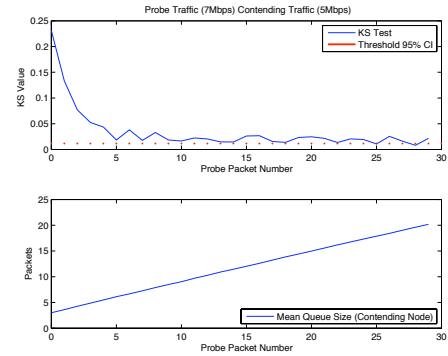


**Figure 5: Analysis of the distribution (7Mbps probe-traffic rate, 5Mbps cross-traffic rate (Top) KS-Test (Bottom) Mean contending node's queue size**

In order to illustrate this evolution first consider the following experiment: using NS2 we send 1000 probe packets at a given rate (5Mbps) and with a static load of contending cross-traffic (4Mbps). We have repeated the experiment 25000 times and, for each probe packet (indexed from 1 to 1000), we compute the distribution of the service delay (considering all the repetitions).

Figure 3 plots the average service delay that each one of the first 150 packets observes. The figure shows how the average service delay perceived by the first packets is lower than for the rest of them. This suggests that, in fact, the distribution of the service delay changes as more probe traffic keeps on arriving to the WLAN link. In order to verify this hypothesis, figure 4 plots the histogram of the service delay as seen by the first probe packet and by the 500th. As the plot shows, the distribution changes significantly. The main rationale behind this is that as new probing packets keep on arriving they keep on increasing the load of the network until reaching a stationary state of interaction with the (contending) cross-traffic.

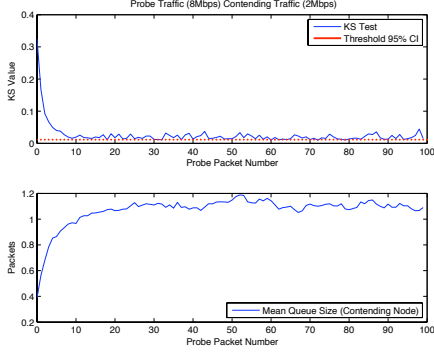


**Figure 6: Analysis of the distribution (8Mbps probe-traffic rate, 2Mbps cross-traffic rate (Top) KS-Test (Bottom) Mean queue size**

Let us focus again on figure 4 (bottom). This histogram plots the distribution of the service delay when the link is saturated. As we can see in the figure, there are 6 visible peaks. These peaks are related to the amount of contending rounds that a probe packet can lose before being successfully transmitted. The first peak is the probability that the probe packets wins the first contending round, the second peak is the probability that loses the first but wins the second and so on. Given the example of 4 (bottom) we could state that, with high probability, a probe packet will need no more than 6 contending rounds to be transmitted. This means that in order to see the distribution figure 4 (bottom) the queue of the contending node must contain around 6 packets, otherwise it will not be possible for a probe packet to require 6 contention rounds to be transmitted. This suggests that the presence and duration of this transitory depends on the queue size of the contending node.

In order to validate this hypothesis we use the well-known Kolmogorov-Smirnov<sup>1</sup> (KS) goodness-of-fit test [15] to compare the resemblance of the delay distribution suffered by every probing packet during the transitory and the delay distribution once probing packets have reached a stationary state. The KS test is non-parametric and analyzes whether two different sets come from the same random distribution. Using this test we compare the distribution of each individual packet in the probing sequence with the service delay distribution of the last 500 probing packets. As mentioned, our hypothesis is that the duration of this transitory regime is related with the queue size of the contending station. Hence we compare the result of the KS-test with the mean queue size of the contending node. The queue size is measured when the probe packet is successfully

<sup>1</sup>Since we are using the KS test to compare two empirical discrete distributions we convert one of them to a continuous one using linear interpolation.

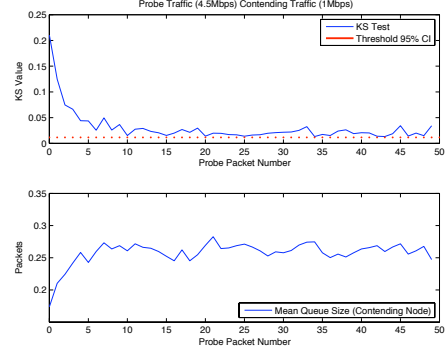


**Figure 7: Analysis of the distribution (4.5Mbps probe-traffic rate, 1Mbps cross-traffic rate (Top) KS-Test (Bottom) Mean contending node's queue size**

transmitted.

Consider the experiment depicted in figure 5 where both probe and cross traffic enter backlog after a certain amount of time. The top plot shows the result of the KS-test on a per probe packet basis. The bottom plot shows the corresponding average queue size at the station that is contending for channel access. It can be seen that the fifth probing packet observes a distribution of service delay that presents a close fit with the stationary distribution (the result of the KS-test approaches the red line that corresponds to the 95% of c.i.). The bottom plot shows how when the fifth probing packet is transmitted the queue size of the contending node reaches 6 packets. This would confirm the hypothesis of the inter-relation between the queue size of the contending node and the stationarity of the service delay of probing packets.

To further validate this hypothesis we repeat the experiment but considering two cases when the contending station does not reach backlog.

First consider the experiment depicted in figure 6. The KS-test plot shows how after 10 probing packets have been transmitted the distribution of the service delay presents a close fit to stationarity (i.e. the KS-test value approaches the 95% threshold). Observing then the queuing evolution of the contending station it can be seen that after the 10th packet is transmitted the queuing length reaches a stable average value around one. Figure 7 presents a similar effect. The difference in this case is that neither the probing station nor the contending node enter backlog at any time. However, the inter-relation between the transitory evolution of the service delay distribution and the number of packets in the queue of the contending node is still evident.

Finally we have also experimented with more complex scenarios. As an example consider figure 8 that shows the KS-test for a case with 4 contending stations using



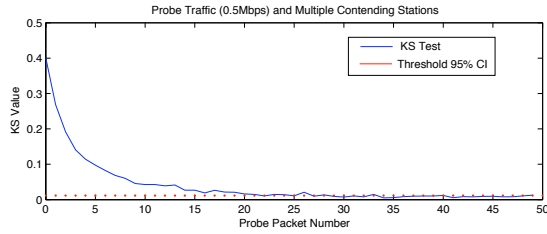


**Figure 8: Analysis of the distribution (complex case)**

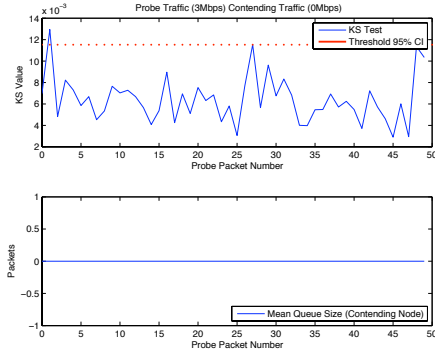


**Figure 9: Analysis of the distribution (3Mbps probe-traffic rate, no contending cross-traffic)**

different packet sizes (40, 576, 1000 and 1500 bytes) and the following rates respectively (0.1, 0.5, 0.75 and 2Mbps). Again the figure reveals a transitory regime in the distribution of the service delay, also related with the queue size of the contending nodes. As the figure shows we need to send tens of packets until reaching a stationary state. We have simulated more cases with different degrees of complexity obtaining similar results. The transitory is present in all the cases that probe traffic has to contend for accessing the air. As a final example consider the experiment depicted in figure 9 where no contending traffic is present. As the figure reveals the transitory is non-existent.

### 3.3 Consequences of the observations

The analysis about the service delay reveals two important issues affecting the bandwidth measurement task.

On one side, the service delay of the probing sequence undergoes a transitory (in distribution) before reaching a stationary state. This implies that the first packets of a probing sequence do not capture the long-term behavior of larger flows and represent biased samples of the stationary interaction between the probing flow and cross-traffic. This observation has a direct impact on bandwidth measurement tools that generally use short trains of packets to support measurements.

On the other side, once reaching the stationary state we can see that the expectation of the service delay

remains stable no matter how many probing packets we inject in the transmission queue (see figure 3). Even more, once contending stations reach a backlog state, no matter how far we increase the probing rate that the service delay distribution remains constant. In WLAN terms, at this point the probing traffic has reached its fair share of the channel and it cannot get a higher piece of it, no matter how hard it tries.

## 4. BASICS OF BANDWIDTH MEASUREMENTS OVER WLANS

This section reviews some of the basic concepts related to bandwidth measurements in the presence of WLAN links. The first part of the section reconsiders bandwidth metrics in the WLAN context. Recent literature [2] suggested that the same metrics that used to be measured in wired environments do not necessarily hold in wireless scenarios. The second part of the section presents rate response curves when placing fluid assumptions over the model of the WLAN introduced in the previous section. This reveals an important result regarding the identifiability of certain metrics in WLAN environments. Fluid curves are later used as a reference for the non-fluid analysis of section 5.

### 4.1 Revisiting bandwidth metrics

Recent literature related to bandwidth measurements in wireless networks has shown how the specific properties of WLAN access techniques compromise the identifiability of traditional bandwidth related metrics. In some cases bandwidth metrics require specific definitions [3, 4] to be measured and in some cases new metrics have been defined to account for the particularities of wireless environments [2].

Traditional metrics associated to bandwidth measurements are *capacity* and *available bandwidth*. On one side, the capacity, as defined in [1], is the maximum possible layer-3 (IP) transfer rate at a given network hop or path. As argued above in a wireless environment, this is a time dependent random process  $C(t)$ . Even more, the value of the *capacity* depends on the point of view of the measurement station (e.g. position, transmission rate, quality of channel, etc.) and strictly depends on the size of the packets used to measure.

On the other side, the *available bandwidth* refers to the portion of the *capacity* that is not being used:  $A(t)$ . As happens with the *capacity* metric, it depends on the point of view of the measurement station and the size of packets being used to measure. Neither the *available bandwidth*, nor the *capacity* can be normalized for all the nodes that contend for channel access. As a result, knowing the amount of cross-traffic (in bits-per-second) that traverses a WLAN link cannot be used to infer the bandwidth available for new stations. Instead, the impact of cross-traffic has to be measured in terms

of the portion of time that the channel is being used. As a consequence, here we take the definition of *available bandwidth* used in [3, 4] where the authors consider that the *available bandwidth* is the maximum rate that a (measurement) node can transmit without affecting the communication of others.

Recent literature related to bandwidth measurement over wireless systems raised some debate around the measurement of *available bandwidth* in WLAN scenarios. In [3] the authors show how traditional techniques fail in measuring such metric in wireless settings. Following such debate and as results in this paper confirm we propose considering the *achievable throughput* metric in relation to traditional bandwidth measurement tools. This metric is not new, it was already defined in [2]. However, the authors proposed an empirical definition of the metric that, as shown here, does not necessarily lead to its actual value. Instead, we propose using the following definition. The rest of the paper uses the term  $B$  to refer to the *achievable throughput*,

$$B = \sup\{r_i : \frac{r_o}{r_i} \geq 1\} \quad (1)$$

In this expression,  $r_i$  is the rate at which a traffic flow enters the path under measurement and  $r_o$  is the rate at which this traffic leaves the path. Therefore, as considered here, the *achievable throughput* is the maximum rate at which we can inject traffic into a network path and still receive traffic at this same rate. The *achievable throughput* is also a time varying metric  $B(t)$  that depends on the specific characteristics of cross-traffic, channel access scheduling and channel propagation. Note that under these definitions the relation between the metrics is  $A(t) \leq B(t) \leq C(t)$  (as stated in [2]). This model assumes that, during the measurement interval, the capacity, the available bandwidth and the achievable throughput are stationary random processes with asymptotic averages  $\bar{C}$ ,  $\bar{A}$  and  $\bar{B}$  respectively.

## 4.2 Bandwidth measurements under fluid assumptions

Here we place fluid assumptions to the WLAN model presented in section 3.1 and review the concept of the rate response curve [13]. The rate response curve relates the rate ( $r_i$ ) of a probing flow when it enters a network path with the rate at the output of the path ( $r_o$ ). Fluid assumptions taken over a wireless link apply to the cross-traffic and to the service rate. Both processes lose their random and time dependent properties under this assumption and become constant over the measurement interval. As a consequence, under fluid assumptions we have that during the entire measurement interval  $A(t) = \bar{A}$ ,  $B(t) = \bar{B}$  and  $C(t) = \bar{C}$ .

Recalling from [13], the fluid rate response curve of a FIFO queue with constant service rate (i.e. the probing

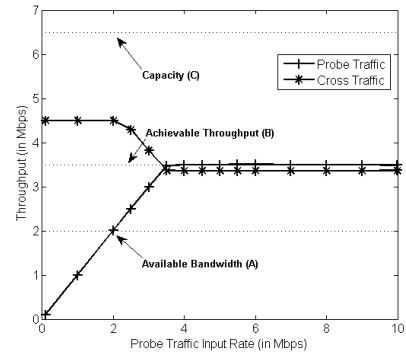


**Figure 10: Experimental fluid rate response curve of probe traffic in a WLAN setting versus throughput of cross-traffic flow.  $C=6.5$ Mbps,  $A=2$ Mbps,  $B=3.4$ Mbps**

and cross-traffic share a FIFO queue) can be expressed as,

$$r_o = \min(r_i, C \frac{r_i}{r_i + C - A}) \quad (2)$$

Note that following our previous discussion we have removed any explicit reference to the amount of cross-traffic *rate* from this expression (usually called  $\lambda$ ) but we rather express the equation from the perspective of the node that is measuring.

It is worth noting also that relating equations 1 and 2 one can see that in a (wired) FIFO system the *achievable throughput*, as defined here, coincides with the *available bandwidth*.

Now let us consider a case when probing packets contend for (wireless) channel access with the cross-traffic such as figure 1 depicts. In this case cross-traffic and probing traffic are not scheduled in FIFO order. Figure 10 plots an experimentation result showing the evolution of the rate response curve when the probing station contends for channel access with another (single) station. In order to obtain the fluid rate response curve we use long packet probing trains (10000 packets). The figure also shows the evolution of the cross-traffic throughput for each probing rate. As it can be seen, when the cross-traffic starts experiencing a decrease in its throughput, that is, when the probing traffic arrives at the available bandwidth ( $\sim 2$ Mbps), the rate response curve shows no sign of deviation (as one would expect from eq. 2). Instead, the rate response curve flattens when the probing rate reaches the fair share ( $\sim 3.5$ Mbps) that it can get from the wireless medium. This fair share corresponds, in fact, to the *achievable throughput* metric defined above.

This observation leads to reformulating eq. 2 for a wireless link as,

$$r_o = \min(r_i, B) \quad (3)$$

Equation 3 is the first conclusion of this paper. The fluid rate-response curve of a wireless link deviates at the *achievable throughput*. Therefore, traditional existing tools based on this curve [1, 17, 18, 19, 20] are, in fact, targeting this metric rather than the *available bandwidth*. Note also that the *available bandwidth* and the *achievable throughput* coincide only when contending stations use a lower portion of the bandwidth than their theoretical fair share.

## 5. NON-FLUID ANALYSIS OF DISPERSION-BASED MEASUREMENTS IN WLANS

Recent studies [13, 14, 16] have taken a non-fluid approach to the bandwidth measurement problem. They reveal that dispersion based measurements of the available bandwidth present fundamental deviations from the fluid model that affect traditional measurement techniques. As they show, such deviations constitute biases that are difficult to remove when the number of packets used to infer bandwidth metrics (the train length) is not large enough.

This section takes a similar approach but applied to bandwidth measurements in WLAN environments.

### 5.1 Analytical framework

Here we present the basic analytical framework used to deal with this problem. This framework was originally proposed in [6] but is extended here to focus on the particularities of WLAN transmissions.

#### 5.1.1 The probing sequence: Arrivals, departures and input gap

The probing sequence consists of a series of  $n$  packets that enter the transmission queue at instants  $\{a_i, i = 1, 2, \dots, n\}$ . Their departure instants, meaning the time at which they are completely transmitted, form the series  $\{d_i, i = 1, 2, \dots, n\}$ . Finally, we are considering here periodic probing flows with a fixed inter-packet arrival time or input gap:  $g_I = a_i - a_{i-1}$ .

#### 5.1.2 The service delay process

As shown above, the service delay that probing packets experience is a random process. This process is the result of the interaction between probing traffic, contending cross-traffic and backoff. To account for this let us define the sequence  $\{\mu_i, i = 1, 2, \dots, n\}$  to denote the random service delay that each one of the  $n$  probing packets of a probing sequence experiences when contending for medium access.

As shown above, the service delay presents a transitory period until reaching a certain stationary distribution. Thus,  $\exists n_0 : \forall \{i > n_0\}, \mu_i$  is i.i.d. Further,

we assume that the service delay distribution is upper and lower bounded. In other words, we assume that  $\exists \{\mu^{max}, \mu^{min}\} : \forall i, Pr(\mu^{min} \leq \mu_i \leq \mu^{max}) = 1$ .

#### 5.1.3 Intrusion residual: amount of probe traffic in the FIFO queue

The intrusion residual  $W_d(t)$  accounts for the sum of the service time of all probing packets in the FIFO queue and the remaining time to service the probing packet that may be in transmission. Next, we define the series  $\{R_i, i = 1, 2, \dots, n\}$  which captures the intrusion residual that every probing packet finds when it enters the transmission queue,

$$R_i(a_1) = W_d(a_i^-) = W_d(a_1 + (i-1)g_I^-) \quad (4)$$

Note<sup>2</sup> that  $R_i$  is a recursive process that under the assumptions in this work can be expressed as,

$$R_i = \begin{cases} 0 & i = 1 \\ \max(0, \mu_{i-1} + R_{i-1} - g_I) & i > 1 \end{cases} \quad (5)$$

Finally, we define the series  $\{Z_i, i = 1, 2, \dots, n\}$  that encloses the queuing plus service delay that each one of the probing packets experiences. Under the assumptions taken,

$$Z_i = d_i - a_i = \mu_i + R_i \quad (6)$$

#### 5.1.4 Dispersion based measurements: The output gap and its relation to the probing rate

Dispersion based measurements of bandwidth metrics consist on measuring the dispersion (or inter-departure time) of packets at the output of a path (receiving side). This measure is then used to infer the value of bandwidth related metrics. The output gap (or dispersion) of a train of probing packets is defined as follows,

$$g_O = \frac{d_n - d_1}{n - 1} \quad (7)$$

Figure 11 illustrates the contribution of the processes defined above to the value of the output gap. From the arrival of the first probing packet at the transmission queue ( $a_1$ ), probing packets keep on arriving at a constant interval of  $g_I$ . The cross-traffic, service delay and the intrusion residual of previous probing packets ( $Z_i$ ) randomize the departure times of probing packets ( $d_i$ ) and thus, their output dispersion ( $g_O$ ).

Observing figure 11 we can obtain the output gap in relation to the different processes involved.

$$g_O = \frac{d_n - d_1}{n - 1} = \frac{(n-1)g_I + Z_n - Z_1}{n - 1} \quad (8)$$

<sup>2</sup>The minus superscript refers to the *a priori* state of the queue.



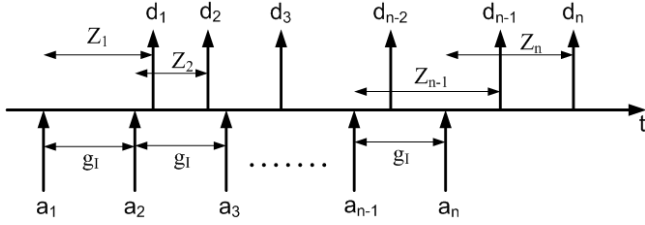


**Figure 11: Inter-relationship between probing arrival sequence ( $a_i$ ), departure sequence ( $d_i$ ) and cross-traffic related processes ( $Z_i$ ).**

Expanding this expression we get the following,

$$g_O = g_I + \frac{R_n}{n-1} + \frac{\mu_n - \mu_1}{n-1} \quad (9)$$

### 5.1.5 Problem formulation

We are interesting in studying whether dispersion measurements can be used to infer the rate response curve of a wireless link. Measurement tools based on dispersion take the assumption that the relation between the input ( $g_I$ ) and output ( $g_O$ ) dispersions of a probing train can be used as estimators of the inter-relation between input ( $r_i$ ) and output ( $r_O$ ) rates of a flow traversing the system. In other words if  $L$  is the length of the packets used for probing, dispersion based measurements assume that  $L/g_I$  is equivalent to  $r_i$  and the same between  $L/g_O$  and  $r_O$ .

Reformulating equation 3, the problem of bandwidth estimation using dispersion measurements can be stated as follows.

$$E[g_O] \stackrel{?}{=} \begin{cases} g_I & g_I \geq \frac{L}{B} \\ \frac{L}{B} & g_I \leq \frac{L}{B} \end{cases} \quad (10)$$

Taking expectation over eq. 9, the rest of this section deals with the evaluation of the behavior of the following expression,

$$E[g_O] = g_I + \frac{E[R_n]}{n-1} + \frac{E[\mu_n] - E[\mu_1]}{n-1} \quad (11)$$

## 5.2 The impact of the randomness of service delay on dispersion measurements

This section studies the impact on dispersion measurements of the randomness of the service delay. Along this section we assume that the service delay does not present the transitory stage described in section 3.2. Instead we assume that, for all probing packets, the service delay is i.i.d. This assumption would apply in a WLAN link with no contending traffic but in which the quality of the channel leads to frequent retransmissions or frequent changes of the transmission rate.

The analysis reveals how dispersion measurements, when taken around the *achievable throughput* present a deviation from the fluid response curve. Interestingly enough the origin of this deviation is similar to the one detected in [13]. This indicates that the randomness of the service delay causes a similar effect as the burstiness of cross-traffic in a (wired) FIFO queue.

### 5.2.1 Expected output dispersion and achievable throughput

Assuming that the service delay does not present the transitory stage detected in section 3.2, expression 11 reduces to the following,

$$E[g_O] = g_I + \frac{E[R_n]}{n-1} \quad (12)$$

Under the assumption of no other (cross-)traffic in the FIFO queue the system can serve, in average, up to one probing packet every  $E[\mu]$ . As a consequence we can state that,

$$\bar{B} = \frac{L}{E[\mu]} \quad (13)$$

### 5.2.2 Expectation on output gap based on bounds of the intrusion residual

From expression 12, we learn that the expected output gap depends on the expected value for the residual that the last packet of the probing train (i.e. with index  $n$ ) finds in the queue. Considering eq. 5 and that the service delay presents upper and lower bounds (i.e.  $\mu^{max}$  and  $\mu^{min}$ ), one can define the following (loose) bounds for the probing residual:

$$\begin{cases} R_n = \sum_{i=1}^{n-1} (\mu_i - g_I) & g_I \leq \mu^{min} \\ \max(0, \sum_{i=1}^{n-1} (\mu_i - g_I)) \leq R_n \leq \sum_{i=1}^{n-1} \mu_i & \mu^{min} \leq g_I \leq \mu^{max} \\ R_n = 0 & g_I \geq \mu^{max} \end{cases} \quad (14)$$

Taking expectation over  $R_n$ , we can identify four differentiated regions,

$$\frac{E[R_n]}{n-1} = \begin{cases} E[\mu] - g_I & g_I \leq \mu_s^{min} \\ \frac{\beta_n}{n-1} & \mu^{min} \leq g_I \leq E[\mu] \\ \frac{\alpha_n}{n-1} & E[\mu] \leq g_I \leq \mu^{max} \\ 0 & g_I \geq \mu^{max} \end{cases} \quad (15)$$

The parameters  $\alpha_n$  and  $\beta_n$  depend on the specific characteristics of the random cross-traffic but can be (loosely) bounded as follows,

$$\begin{cases} E[\mu] - g_I \leq \frac{\beta_n}{n-1} \leq E[\mu] \\ 0 \leq \frac{\alpha_n}{n-1} \leq E[\mu] \end{cases} \quad (16)$$

Finally, we are interested in the output dispersion. Thus, substituting eq. 15 into eq. 12 we get the following,

$$E[g_O] = \begin{cases} E[\mu] & g_I \leq \mu^{\min} \\ g_I + \frac{\beta_n}{n-1} & \mu^{\min} \leq g_I \leq E[\mu] \\ g_I + \frac{\alpha_n}{n-1} & E[\mu] \leq g_I \leq \mu^{\max} \\ g_I & g_I \geq \mu^{\max} \end{cases} \quad (17)$$

Two important observations about eq. 17 are that, first,  $\alpha_n$  and  $\beta_n$  are deviation terms that depend on the length of the packet train ( $n$ ) and that disappear when the input gap ( $g_I$ ) falls outside the limits of the random service delay. Second, the lower bound of the output gap corresponds to the fluid response curve.

### 5.2.3 Numerical results on the rate response curve

In order to obtain numerical evidence of the expressions presented above we have used the queuing simulator introduced in section 2. Figure 12 plots the expected rate response curve inferred using the dispersion of probing trains of different lengths (2, 10 and 20 packets) at the output of a system with exponentially distributed service delay (see [6]). The mean service delay that probing packets experience corresponds to an achievable throughput of 3.5Mbps (probing packets are 1500 bytes long). The fluid response curve is also included. The figure shows how when probing around the *achievable throughput* dispersion measurements deviate from the fluid response curve. The deviation is higher the lower the number of packets used to measure. The figure plots also, as a reference, the (lower) bound on the maximum deviation of the rate response curve coming from the (upper) bound on the expected output gap derived in expression 17.

### 5.2.4 The origin of the bias

The biases detected in eq. 17 and shown in figure 12 have their origin in the evolution of the expected queuing delay that probing packets suffer when traversing the transmission queue before being served (see 2 for a reference). To illustrate this, figure 13 plots, for various probing rates, the difference in the mean delay experienced by each one of the first 100 packets of a long probing flow with respect to their immediate predecessor. In other words it plots the process  $\{E[Z_i - Z_{i-1}], i = 2, \dots, n\}$ . It can be seen from the figure that it takes some probing packets until the process  $E[Z_i - Z_{i-1}]$  becomes stable (constant). This is precisely what deviates the  $\alpha_n$  and  $\beta_n$  terms in equation 16 from the fluid response curve.

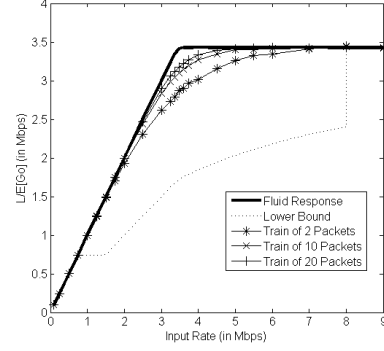


**Figure 12: Rate response curve when probing a system with exponentially distributed service delay with probing sequences of different length.**

This figure reveals that, when probing packets are served with random delay, it takes some packets until they start experiencing a stationary behavior. The first packets, then, constitute biased measures of the delay required to traverse the link. In other words, first packets are not able to capture the stationary behavior of the queue state and distort dispersion measurements.

### 5.2.5 Asymptotics of the deviation terms

As figure 13 suggests, the longer the packet train the lower the bias of dispersion measurements. It can be shown that eq. 17 tends asymptotically to the fluid response curve as  $n$  increases. That is,

$$\lim_{n \rightarrow +\infty} \frac{\alpha_n}{n-1} = 0 \quad (18)$$

and,

$$\lim_{n \rightarrow +\infty} \frac{\beta_n}{n-1} = E[\mu] - g_I \quad (19)$$

Furthermore, if we unbound the service delay, it can be shown that there exists a strong relation between the variance of the service delay and the intensity of the deviation of dispersion measurements from the rate response curve. We have that,

$$\lim_{Var[\mu] \rightarrow +\infty} \frac{\alpha_n}{n-1} = E[\mu] \quad (20)$$

and,

$$\lim_{Var[\mu] \rightarrow +\infty} \frac{\beta_n}{n-1} = E[\mu] \quad (21)$$

### 5.2.6 A final remark

The findings in this section present high similarities with the ones presented in [13]. This indicates that the

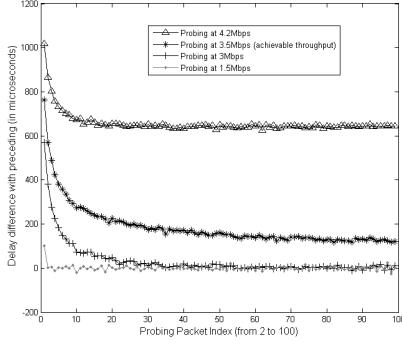


**Figure 13: Expected per-packet delay difference between consecutive probing packets sent through a FIFO queue with exponential service delay**

impact on probing traffic of a random service delay process (i.i.d) is similar to the case when probing packets share a (wired) FIFO queue with a bursty cross-traffic flow.

### 5.3 The impact of the transitory regime of service delay on dispersion measurements

This section reintroduces the transitory of the service delay and studies its impact on dispersion measurements.

The basic finding here is that the transitory of the service delay induces new deviations of the rate response curve, but in the opposite direction than the pure i.i.d random service. As a consequence packets in short probing trains are 'accelerated' in comparison to packets in longer trains. This may lead to obtaining overestimates of the actual rate response curve when using dispersion measurements.

#### 5.3.1 Expected output dispersion and achievable throughput

Now the expression of the output gap cannot be reduced and our objective is studying this expression,

$$E[g_O] = g_I + \frac{E[R_n]}{n-1} + \frac{E[\mu_n] - E[\mu_1]}{n-1} \quad (22)$$

We can define again a relation between the achievable throughput and the service delay that probing packets receive.

$$\frac{L}{B} = \frac{1}{n} \sum_{i=1}^n (E[\mu_i]) \quad (23)$$

Note also that as the number of probing packets grows the expected service delay becomes constant and we can say that,

$$\frac{L}{B} \xrightarrow{n} E[\mu_n] \quad (24)$$

#### 5.3.2 Expectation on output gap based on bounds of the intrusion residual

Following similar reasoning as in the previous section, the expected output dispersion of a train of  $n$  packets presents four differentiated regions such as,

$$E[g_O] = \begin{cases} \frac{1}{n-1} (\sum_{i=2}^n (E[\mu_i])) & g_I \leq \mu^{min} \\ g_I + \frac{\beta_n}{n-1} & \mu^{min} \leq g_I \leq \frac{1}{n} \sum_{i=1}^n E[\mu_i] \\ g_I + \frac{\alpha_n}{n-1} & \frac{1}{n} \sum_{i=1}^n E[\mu_i] \leq g_I \leq \mu^{max} \\ g_I + \frac{[\mu_n - \mu_1]}{n-1} & g_I \geq \mu^{max} \end{cases} \quad (25)$$

The parameters  $\alpha_n$  and  $\beta_n$  in the expression above are bounded as follows,

$$\begin{cases} \frac{1}{n} \sum_{i=2}^n (E[\mu_i] - g_I) \leq \frac{\beta_n}{n-1} \leq \frac{1}{n-1} \sum_{i=2}^n (E[\mu_i]) \\ 0 \leq \frac{\alpha_n}{n-1} \leq \frac{1}{n-1} \sum_{i=2}^n (E[\mu_i]) \end{cases} \quad (26)$$

Expressions 25 and 26 reveal some interesting features about dispersion measurements for WLAN environments.

First, note that considering that the expected service delay in a WLAN environment is an increasing function with respect to the packet index ( $i$ ), the following is true for any value of  $n$ ,

$$\frac{1}{n-1} \sum_{i=2}^n (E[\mu_i]) < E[\mu_n] \quad (27)$$

As a result, when probing packets arrive faster than the achievable throughput (i.e.  $g_I \leq \frac{1}{n} \sum_{i=1}^n E[\mu_i]$ ), packets at the output experience a 'compression' effect with respect to the fluid response that leads to inferring higher output rates than those that can be actually achieved in this region.

Second, as eq. 26 reveals, the upper bound of  $\alpha_n$  is lower than without the presence of the transitory. The bias introduced by this term in dispersion measurements is, thus, lower than would be expected without the presence of the transitory.

Third, when the input rate is low enough (i.e. when  $g_I \geq \mu^{max}$ ) the transitory causes an expansion of the expected output dispersion. This effect is hidden in rate response curves

Figure 14 shows an experimental result showing these observations. The rate response curves plotted correspond to those of packet trains probing a WLAN link at different rates. The figure clearly shows how, when short packet trains are used, the rate response curve gathered leads to inferring higher rates than the achievable throughput. The figure also shows how the bias in-

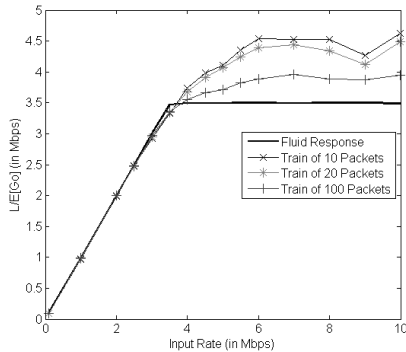


Figure 14: Experimental rate response curve when probing a WLAN system with probing sequences of different length

roduced by the  $\alpha_n$  term and the expansion suffered at low probing rates are not important enough to distort the measurement process.

## 6. DISCUSSION ON CONSEQUENCES AND APPLICATIONS OF FINDINGS

This section discusses the main findings of this study and some consequences and possible applications that they entail.

### 6.1 Summary of findings

- In section 4 we showed how the rate response curve, when applied over a WLAN system, presents a deviation point at the *achievable throughput* rather than the *available bandwidth*
- In section 5 we showed how dispersion based measurements are biased estimations of the rate response curve. There are two possible sources of bias in a WLAN system. On one side there is the randomness of the service delay that probing packets may experience. On the other side, there is the transitory in distribution that the random service delay presents when probing traffic contents for channel access. In both cases the origin of the bias lies in the fact that it takes a while (some packets) for the probing traffic to completely interact with the system. This implies that the first packets in a probing sequence are not valid samples of the stationary behavior of the system.

### 6.2 A consequence: bandwidth estimation in WLAN links

As shown in section 4, traditional methodologies developed taking the rate response curve as a reference target the *achievable throughput* rather than the *available bandwidth*. The same happens with those tools

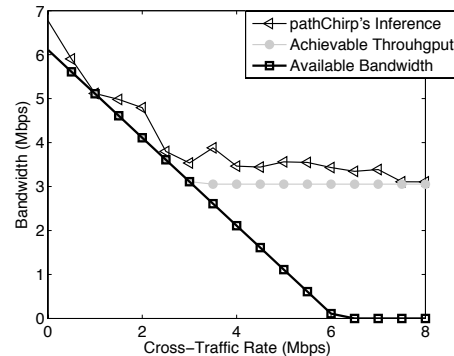


Figure 15: Estimation of pathChirp in a wireless link (1 contending node, exponential inter-departure time, 1500bytes as packet size, intensity varies). The tool follows the achievable throughput rather than the available bandwidth.

designed to infer the *capacity* based on dispersion measurements.

At this point arises the question of whether it is worth measuring the *achievable throughput* of a network path. We argue that such a metric can be useful for routing protocols, overlay/P2P network formations or even in congestion control algorithms as it allows knowing the throughput that a given node will receive when sending data without distortion. As an example, for TCP congestion control, it would allow maintaining a more efficient control of the evolution of the congestion window during the congestion avoidance phase. However, the *available bandwidth* metric is still of much interest for applications such as access control algorithms or to tune the slow start phase of TCP congestion control. As shown in section 4 however, the rate response curve does not present any signal at the available bandwidth and novel methodologies such as the one proposed in [3] should be developed.

To illustrate this consider the experiment depicted in figure 15 (NS2). We have run a state-of-the-art available bandwidth estimation tool (pathChirp [19]) in the presence of a wireless link. This tool is designed with the rate response curve as a reference and tries to find a turning point in the curve using dispersion of packets. As the figure shows pathChirp points at the *achievable throughput*. This becomes clear when the available bandwidth and achievable throughput deviate one from the other (at around 3Mbps in this case).

### 6.3 Another consequence: packet pair measurements in WLAN links

A common approach to measure the capacity of a network path is the packet-pair technique[23]. Recently, packet pairs have gained momentum as they have been extensively used to develop routing metrics in all-wireless

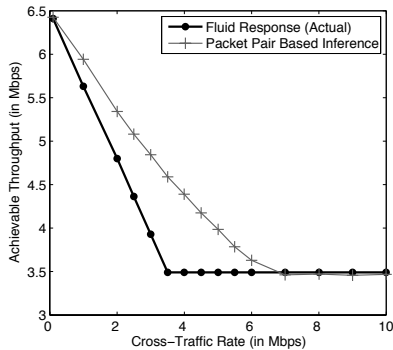


**Figure 16: Experimental comparison between packet pair based bandwidth measurements and the actual fluid response in a WLAN link**

multi-hop networks [21].

However, as a consequence of the results presented in section 4, packet pairs (understood as probes of infinite rate) target the *achievable throughput* when used in a WLAN link. Even more, considering results from section 5.3, one can see that packet pairs tend to overestimate the value of the *achievable throughput*. Figure 16 illustrates this fact. It plots the actual *achievable throughput* of a WLAN link and the estimation using average dispersion of packet-pairs. This is done for different levels of cross-traffic. The *capacity* of the WLAN link is kept constant for all the measurement process at 6.5Mbps (no channel propagation errors). As one can see the packet-pair does not measure the *capacity* in the whole measurement region except when no contending traffic is present.

#### 6.4 An application of results: improving the convergence and accuracy of traditional tools

The results presented in section 5 entail a second important observation that can be used to improve the accuracy of bandwidth measurement tools. As figure 3 and 13 reveal, the first packets that traverse a WLAN link constitute non-accurate samples of the stationary behavior. A direct implication of this is that first samples (packets) of the probing train should be removed from bandwidth estimates as they are not accurate.

Traditionally the approach to remove measurement biases consists in enlarging the number of packets used to gather measurements. However, this comes at the cost of increasing the intrusiveness of the measurement process over the measured path. The results in section 5 lead to the observation that removing the first packet samples from bandwidth measurements helps reducing the measurement bias and can help improve the measurement accuracy with a limited number of probing packets.

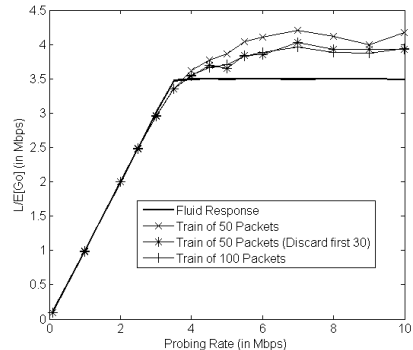


**Figure 17: Experimental rate response curves showing the bias incurred by different probing strategies**

Figure 17 illustrates this observation. As the figure shows one can achieve the same measurement accuracy using trains of 50 packets (but removing the first 30 from the measure) as when using trains of 100 packets. This could be easily applied to existing tools [1, 17, 18, 19, 20, 22, 23] improving their accuracy and/or reducing their convergence time.

Interestingly enough, the similarity of results in section 5.2 and the results presented in [13] suggests that removing the first packets from measurements of *available bandwidth* taken over wired paths would also increase the accuracy of the result.

## 7. CONCLUSIONS

This paper presents a study of the bandwidth measurement problem over WLANs. The paper models the time to service probing packets as a random process and analyzes the interaction between periodic probing sequences and this random process. The approach is non-parametric.

The analysis reveals how the randomness of the WLAN service time introduces a bias in measurement techniques based on the dispersion of probing packets. Interestingly, this bias presents strong similarities with the one reported in [13, 14] which suggests that bursty cross-traffic can be assimilated as any other random process affecting a periodic probing sequence. Hence, the results presented here can be made extensible to any other system containing any form of randomness in the time to transmit packets (e.g. PLC links). Further, for the particular case of an IEEE 802.11 link, the paper reveals that the service delay does not follow a stationary process but, instead, presents a transitory regime. This transitory introduces additional bias in bandwidth measurements which lead to an overestimation of the rate-response curve of a WLAN link when probing at high packet rates.

Several important problems remain open for future work. First this analysis, as well as [13, 14], focuses on periodic probing sequences. Extending this analysis to other probing processes such as Poisson may lead to interesting conclusions. Alternative probing sequences present also the same transitory behavior as periodic probing sequences and may also be subject to similar biases. Second, we have seen that dispersion measurements are not useful to measure the *available bandwidth*. Therefore, it would be interesting to explore whether other mechanisms can be used for this purpose.

## 8. REFERENCES

- [1] R.S.Prasad et al. "Bandwidth Estimation: Metrics, Measurement Techniques and Tools", IEEE Network 2003
- [2] Mingzhe Li et al. "Packet Dispersion in IEEE 802.11 Wireless Networks", in Proc. of IEEE Local Computer Networks 2006
- [3] Karthik Lakshminarayanan, "Bandwidth Estimation in Broadband Access Networks" In Proc. of the ACM SIGCOMM conference on Internet measurement (IMC), 2004
- [4] Andreas Johnsson et al. "An Analysis of active end-to-end bandwidth measurements in wireless networks" In Proc. of IEEE E2EMon 2006
- [5] Issariyakul T. et al., "Exact Distribution of Service Delay in IEEE 802.11 DCF MAC", In Proc. of Global Telecommunications Conference (GLOBECOM), 2005
- [6] Shahrokh Valaee, "Bandwidth Estimation and Distributed Traffic Regulation in Wireless Local Area Networks" In Proc. of the Personal, Indoor and Mobile Radio Communications (PIMRC), 2008
- [7] de A. Rocha, et al. "An End-to-End Technique to Estimate the Transmission Rate of an IEEE 802.11 WLAN" In Proc. of IEEE ICC 2007
- [8] G. Bianchi, "Performance Analysis of the IEEE 802.11 Distributed Coordination Function" IEEE Journal on Selected Areas in Communications, Vol. 18, Num. 3, 2000
- [9] Marc Portoles-Comeras et al. "EXTREME: Combining the ease of management of multi-user experimental facilities and the flexibility of proof of concept testbeds" In proc. of the IEEE TridentCom, 2006
- [10] Multi-Generator (MGEN) (online) <http://cs.itd.nrl.navy.mil/work/mgen/>
- [11] Attila Pásztor and Darryl Veitch, "PC Based precision timing without GPS" SIGMETRICS Perform. Eval. Rev. Vol. 30, Num. 1, 2002
- [12] The Network Simulator NS2 (online) <http://www.isi.edu/nsnam/ns/>
- [13] Liu X., Ravindran K., Liu B., and Loguinov, D., "A Queuing-Theoretic Foundation of Available Bandwidth Estimation: Single-Hop Analysis" IEEE/ACM Transactions on Networking, Vol. 15, Num. 6, 2007
- [14] X. Liu, K. Ravindran, and D. Loguinov, "Multi-Hop Probing Asymptotics in Available Bandwidth Estimation: Stochastic Analysis," In Proc. of USENIX/ACM IMC, October 2005.
- [15] NIST/SEMATECH e-Handbook of Statistical Methods (online) [http://www.itl.nist.gov/div898/handbook/\(Sec. 1.3.5.6\)](http://www.itl.nist.gov/div898/handbook/(Sec.1.3.5.6))
- [16] P.Haga, K. Diriczi et al, "Granular model of packet pair separation in Poissonian traffic" Elsevier Computer Networks, Vol. 51, Num. 3, 2006
- [17] M. Jain et al. "End-to-End Available Bandwidth: Measurement Methodology, Dynamics and Relation with TCP Throughput", In Proc of ACM Sigcomm 2002
- [18] N. Huet et al. "Evaluation and Characterization of Available Bandwidth Techniques" IEEE JSAC 2003
- [19] V. J. Ribeiro, R. H. Riedi, R. G. Baraniuk, J. Navratil, and L. Cottrell, "pathChirp: Efficient available bandwidth Estimation for Network Paths" In Proceedings of Passive and Active Measurements (PAM), 2003
- [20] J. Strauss, "A Measurement Study of available bandwidth Estimation tools" In Proc. of the ACM SIGCOMM conference on Internet measurement (IMC), 2003
- [21] R. Draves et al. "Routing in Multi-Radio, Multi-Hop Wireless Mesh Networks" In Proc. of ACM Mobicom 2004
- [22] Albert Cabellos-Aparicio et al., "A Novel Available Bandwidth Estimation and Tracking Algorithm", in Proc. of IEEE E2EMon 2008
- [23] Dovrolis C., Ramanathan P., and Moore, D. "Packet dispersion techniques and a capacity estimation methodology" IEEE/ACM Transaction on Networking, Vol. 12, Num. 6, 2004
- [24] Marc Portoles-Comeras et al., "Framework for characterizing hardware deployed in wireless mesh networking testbeds" In Proc. of Tridentcom 2007